RM L52K14a

NACA

RESEARCH MEMORANDUM

AN ANALYSIS OF THE LATERAL STABILITY OF THE DOUGLAS D-558-II AIRPLANE EQUIPPED WITH A YAW DAMPER, WITH SPECIAL REFERENCE TO THE EFFECT OF YAW-DAMPER RATE-GYRO SPIN-AXIS ORIENTATION

By Ordway B. Gates, Jr., Albert A. Schy,
and C. H. Woodling

Langley Aeronautical Laboratory
Langley Field, Va.

NATIONAL ADVISORY COMMITTEE
FOR AERONAUTICS

WASHINGTON

March 16, 1953
Declassified May 8, 1957

NACA RM L52K14a

NATIONAL ADVISORY COMMITTEE FOR AERONAUTICS

RESEARCH MEMORANDUM

AN ANALYSIS OF THE LATERAL STABILITY OF THE DOUGLAS D-558-II AIRPLANE EQUIPPED WITH A YAW DAMPER, WITH SPECIAL REFERENCE TO THE EFFECT OF YAW-DAMPER RATE-GYRO SPIN-AXIS ORIENTATION

By Ordway B. Gates, Jr., Albert A. Schy, and C. H. Woodling

SUMMARY

A theoretical investigation has been made to determine the effect of a yaw damper on the lateral stability of the Douglas D-558-II airplane for various anticipated flight conditions. Since the airplane angle of attack varies considerably with changes in flight condition, the inclination of the rate-gyro spin axis is very important in determining the stabilizing effect of the yaw damper. Possible advantages of orienting the gyro spin axis in the direction of the airplane Y-axis are considered. A combination of yaw-damper gearing ratio and yaw-damper axes inclination is selected so that the airplane has satisfactory Dutch roll stability for the flight conditions considered. These flight conditions were cruising at a Mach number of 1.6 at 50,000 feet and 70,000 feet in 1g flight, at the same altitudes and Mach number in 2g flight, and landing at two different lift coefficients.

A particular auxiliary control surface is recommended for use with the damper, and theoretical estimates are presented of the aerodynamic characteristics of the proposed surface. The results of the investigation indicated that a combination of gearing ratio and yaw-damper inclination can be selected so that the lateral stability characteristics of the Douglas D-558-II should be satisfactory in all the flight conditions considered.

INTRODUCTION

Recent flight tests of the Douglas D-558-II research airplane have indicated that the lateral or Dutch roll oscillation of this airplane is very poorly damped. At present, the undesirable stability characteristics of the airplane in the cruising or clean condition at supersonic Mach numbers are of primary interest since these characteristics must be improved before the airplane can reach the speeds of which it is potentially capable. Also, some difficulty has been experienced in the landing condition. A yaw damper has been designed and constructed by the Flight Research Division of the Langley Aeronautical Laboratory and, when installed in the airplane, it should markedly improve the poor

Dutch roll stability of the Douglas D-558-II. Briefly, this system will cause an auxiliary surface to be deflected proportional to the airplane rate of yaw in such a manner as to damp the lateral motions of the airplane. A previous analysis of the effects of a yaw damper on the stability of the Douglas D-558-II has been reported in reference 1, but the present investigation makes use of stability derivatives obtained from recent wind-tunnel tests at both subsonic and supersonic speeds and, in addition, takes into consideration the actual characteristics of the yaw damper.

The purpose of this paper is to determine by theoretical analysis the effects of the proposed yaw damper on the lateral stability of the Douglas D-558-II for several representative flight conditions of the airplane and to recommend, on the basis of these effects, a gearing ratio (control deflection per unit rate of yaw) and an inclination of the rate gyro Z-axis to the airplane Z-axis such that the poor damping of the airplane lateral oscillation will be satisfactorily improved. The term "satisfactory damping," as used in this paper, implies that the lateral oscillation damps to one-half amplitude in one cycle or less. This is an arbitrary value which was chosen for convenience in the calculations and is somewhat more rigid than the Air Force criterion (ref. 2) for satisfactory damping over the range of frequencies of the Douglas D-558-II. In addition, attention is given to the design and location of the control surface which is to be actuated by the yaw damper, since the surface characteristics will have a direct bearing on the selection of a suitable gearing ratio for the yaw damper.

The results of this analysis are presented in the form of stability boundaries and airplane motions for the various flight conditions. The motions were calculated on a Reeves Electronic Analog Computer.

SYMBOLS AND COEFFICIENTS

ϕ	angle of roll, radians
ψ	angle of yaw, radians
β	angle of sideslip, v/V, radians
$r, \dot{\psi}$	yawing angular velocity, $d\psi/dt$, radians/sec
$p, \dot{\phi}$	rolling angular velocity, $d\phi/dt$, radians/sec
$\dot{\theta}$	pitching angular velocity, $d\theta/dt$, radians/sec
v	sideslip velocity along lateral axis, ft/sec, radians/sec

V	airspeed, ft/sec
M	Mach number
M_y	pitching moment of gyro about gyro Y-axis
ρ	mass density of air, slugs/cu ft
q	dynamic pressure, $\frac{1}{2}\rho V^2$, lb/sq ft
b	wing span, ft
S	wing area, sq ft
W	weight of airplane, lb
m	mass of airplane, W/g, slugs
g	acceleration due to gravity, ft/sec^2
μ_b	relative-density factor, $m/\rho Sb$
ϵ	angle between longitudinal body axis and principal axis, positive when body axis is above principal axis at the nose, deg
η	inclination of principal longitudinal axis of airplane with respect to flight path, positive when principal axis is above flight path at nose, $\alpha - \epsilon$, deg
γ	angle of flight path to horizontal axis, positive in a climb, deg
I_{X_o}	airplane moment of inertia about principal X-axis, $I_{X_o} = mk_{X_o}^2$, slug-ft^2
I_{Z_o}	airplane moment of inertia about principal Z-axis, $I_{Z_o} = mk_{Z_o}^2$, slug-ft^2
I_{Y_G}	gyro moment of inertia about gyro Y- or gimbal axis
I_{X_G}	gyro moment of inertia about gyro X- or spin axis

k_{X_o} radius of gyration in roll about principal longitudinal axis, ft

k_{Z_o} radius of gyration in yaw about principal vertical axis, ft

K_{X_o} nondimensional radius of gyration in roll about principal longitudinal axis, k_{X_o}/b

K_{Z_o} nondimensional radius of gyration in yaw about principal vertical axis, k_{Z_o}/b

K_X nondimensional radius of gyration in roll about longitudinal stability axis, $\sqrt{K_{X_o}{}^2\cos^2\eta + K_{Z_o}{}^2\sin^2\eta}$

K_Z nondimensional radius of gyration in yaw about vertical stability axis, $\sqrt{K_{Z_o}{}^2\cos^2\eta + K_{X_o}{}^2\sin^2\eta}$

K_{XZ} nondimensional product-of-inertia parameter, $\left(K_{Z_o}{}^2 - K_{X_o}{}^2\right)\sin\eta\cos\eta$

C_L trim lift coefficient, $\frac{W\cos\gamma}{qS}$

C_l rolling-moment coefficient, $\frac{\text{Rolling moment}}{qSb}$

C_n yawing-moment coefficient, $\frac{\text{Yawing moment}}{qSb}$

C_Y lateral-force coefficient, $\frac{\text{Lateral force}}{qS}$

$C_{l_\beta} = \frac{\partial C_l}{\partial \beta}$

$C_{n_\beta} = \frac{\partial C_n}{\partial \beta}$

$$C_{Y_\beta} = \frac{\partial C_Y}{\partial \beta}$$

$$C_{n_r} = \frac{\partial C_n}{\partial \frac{rb}{2V}}$$

$$C_{n_p} = \frac{\partial C_n}{\partial \frac{pb}{2V}}$$

$$C_{l_p} = \frac{\partial C_l}{\partial \frac{pb}{2V}}$$

$$C_{Y_p} = \frac{\partial C_Y}{\partial \frac{pb}{2V}}$$

$$C_{Y_r} = \frac{\partial C_Y}{\partial \frac{rb}{2V}}$$

$$C_{l_r} = \frac{\partial C_l}{\partial \frac{rb}{2V}}$$

t	time, sec
D	differential operator, d/dt
P	period of oscillation, sec
$T_{1/2}$	time for amplitude of oscillation or aperiodic mode to change by factor of 2; positive value indicates damping, negative value indicates divergence
$C_{1/2}$	cycles to damp to one-half amplitude, $\frac{T_{1/2}}{P}$
a	real part of complex root of characteristic stability equation
ω	angular frequency, radians/sec

ω_o yaw-damper natural frequency, radians/sec

ξ yaw-damper damping ratio

$\lambda = a \pm i\omega$

δ_A deflection of the auxiliary control surface, radians

δ_{ps} deflection of pump servo arm (see fig. 1)

$C_{n_{\delta_A}}, C_{l_{\delta_A}}$ control effectiveness parameters, $\frac{\partial C_n}{\partial \delta_A}; \frac{\partial C_l}{\partial \delta_A}$

α_o angle of attack of longitudinal body axis to flight path, deg (see fig. 2)

X_G rate-gyro spin axis

Y_G rate-gyro gimbal axis

Z_G rate-gyro axis normal to spin and gimbal axes

Φ inclination of rate-gyro Z_G-axis to the airplane Z-axis, deg (see fig. 2)

κ_o angle between rate-gyro Z_G-axis and flight-path Z-axis when airplane is undisturbed, deg (see fig. 2)

δ_G angular displacement of rate-gyro spin axis about gyro Y- or gimbal axis due to airplane angular velocity about rate-gyro Z-axis, deg (see fig. 2)

κ inclination of rate-gyro Z-axis to flight-path Z-axis; ($\kappa = \kappa_o + \delta_G$ when gyro spin axis is oriented in the direction of airplane X-axis; $\kappa = \kappa_o$ when oriented in the direction of airplane Y-axis), deg

$\ddot{\sigma}$ airplane acceleration about gyro Y- or gimbal axis, radians/sec^2

$\dot{\psi}_B$ yawing velocity about airplane Z-axis, $\dot{\psi}_s \cos \alpha_o + \dot{\phi}_s \sin \alpha_o$, radians/sec

$\dot{\psi}_G$ yawing velocity about an axis perpendicular to the gyro spin axis, $\dot{\psi}_S \cos \kappa + \dot{\phi}_{SA} \sin \kappa$, radians/sec

M_{pr} gyro precessional moment due to airplane rate of yaw about gyro Z_G-axis

M_{δ_G} gyro restoring moment due to gyro deflection, $\partial M_y / \partial \delta_G$

$M_{\dot{\delta}_G}$ gyro damping moment due to rate-of-gyro deflection, $\partial M_y / \partial \dot{\delta}_G$

M_f moment about gyro gimbal axis due to Coulomb friction

ω_{X_G} rotational velocity of gyro about gyro spin axis, radians/sec

K_o gearing ratio of yaw damper, $\left| \delta_A / \dot{\psi}_G \right|$

K gearing ratio, $\left| \delta_A / \delta_G \right|$

τ servo time constant

$\frac{l}{b}$ nondimensional distance from center of gravity of airplane to center of pressure of auxiliary control surface

$\frac{h}{b}$ nondimensional distance from airplane longitudinal body axis to center of pressure of auxiliary control surface

Subscripts:

G gyro axis

S stability axis

B airplane body axis

A auxiliary control surface

DESCRIPTION OF THE PROPOSED YAW DAMPER AND AUXILIARY SURFACE

Yaw Damper

The proposed yaw damper consists of a spring-restrained gyro which is deflected proportional to the airplane rate of yaw about the gyro Z-axis and a hydraulic servoactuator which deflects an auxiliary control surface proportional to the rate-gyro spin-axis deflection. A sketch of the system is presented in figure 1 and the system of axes employed in the analysis is shown in figure 2. Briefly, when the airplane experiences a rate of yaw about the gyro Z_G-axis, a precessional moment M_{pr} is applied to the gyro which is equal to the product of the gyro moment of inertia about its spin axis, the angular velocity of the gyro, and the airplane rate of yaw about the gyro Z-axis; that is,

$$M_{pr} = I_{X_G}\omega_{X_G}\dot{\psi}_G \tag{1}$$

The differential equation which describes the gyro spin-axis deflection subsequent to an applied moment is

$$\left(I_{Y_G} D^2 - M_{\dot{\delta}_G} D - M_{\delta_G}\right)\delta_G = M_y - I_{Y_G}\ddot{\sigma} - \text{sign } D\delta \times M_f \tag{2}$$

where I_{Y_G} is the moment of inertia of the gyro about its Y-axis, $M_{\dot{\delta}_G}$ is a measure of the gyro viscous damping, M_{δ_G} is the spring constant of the restraining springs, M_f is the moment due to Coulomb friction (the notation "sign $D\delta$" is used to point out that this moment always opposes the gyro rate of deflection), M_Y is any applied moment about the gyro Y-axis, which for the problem being considered is that moment defined by equation (1), and $\ddot{\sigma}$ is the airplane angular acceleration about the gyro Y-axis; hence,

$$\left(I_{Y_G} D^2 - M_{\dot{\delta}_G} D - M_{\delta_G}\right)\delta_G = I_{X_G}\omega_{X_G}\dot{\psi}_G - I_{Y_G}\ddot{\sigma} - \text{sign } D\delta \times M_f \tag{3}$$

The moment due to Coulomb friction M_f has been measured and found to be approximately 0.33 inch-pound. The minimum value of $\dot{\psi}_G$, based on this value of M_f, below which the system will be insensitive is about

$1/4^{\circ}$ per second. Since this value is small, M_f is assumed to be zero throughout the analysis to follow. The angular velocity of the airplane about the gyro Z-axis is related to the airplane yawing and rolling velocities about stability axes by the following expression:

$$\dot{\psi}_G = \dot{\psi}_s \cos \kappa + \dot{\phi}_s \sin \kappa \tag{4}$$

where κ is the angle between the stability Z-axis and the gyro Z-axis. If the gyro spin axis is oriented in the direction of the airplane X-axis, the angle κ will vary, since the gyro is deflected about its gimbal axis (gyro Y-axis) due to airplane yawing about the gyro Z-axis. If, however, the gyro spin axis is oriented in the direction of the airplane Y-axis, the angle κ is essentially independent of the gyro deflection; hence, in the discussion to follow both orientations are considered.

Gyro spin axis oriented in direction of airplane X-axis (fig. 2(a)).- For this orientation, κ may be defined as follows:

$$\kappa = \kappa_o + \delta_G$$

where κ_o is the angle between the gyro Z-axis and the stability Z-axis when $\dot{\psi}_G = 0$, and δ_G is the gyro deflection about its Y- or gimbal axis due to airplane yawing about the gyro Z-axis. The angle κ_o varies from one flight condition to another since it is dependent upon the airplane trim angle of attack. The angularity between the gyro Z-axis and the airplane-body Z-axis (subsequently referred to as Φ) is set on the ground and does not vary as the flight condition is changed; thus, κ_o is defined as

$$\kappa_o = \alpha_o - \Phi$$

Then, κ becomes

$$\kappa = \left(\alpha_o - \Phi\right) + \delta_G$$

and, for the assumption that the cosine and sine of a small angle are approximately equal to unity and to the angle in radians, respectively,

$$\dot{\psi}_G = \dot{\psi}_s + \left(\alpha_o - \Phi\right)\dot{\phi}_s + \delta_G\dot{\phi}_s \tag{5}$$

Thus, when the gyro spin axis is oriented in the direction of the airplane X-axis, $\dot{\psi}_G$ is a nonlinear function of $\dot{\psi}_s$ and $\dot{\phi}_s$ due to the term $\delta_G\dot{\phi}_s$.

Gyro spin axis oriented in direction of airplane Y-axis (fig. 2(b)).- If the spin axis of the rate gyro is oriented so that it is coincident with the airplane Y-axis when $\dot{\psi}_G = 0$ and if the gyro Z-axis is tilted at an angle Φ to the airplane Z-axis, then the angular velocity of the airplane about the gyro Z-axis is given as

$$\dot{\psi}_G = \dot{\psi}_{[G]_{\delta_G=0}} \cos \delta_G + \dot{\theta} \sin \delta_G \tag{6}$$

where $\dot{\psi}_{[G]_{\delta_G=0}}$ is the yawing velocity of the airplane about an axis which is coincident with the gyro Z-axis when $\delta_G = 0$ and $\dot{\theta}$ is the airplane pitching velocity. The expression for $\dot{\psi}_{[G]_{\delta_G=0}}$ is

$$\dot{\psi}_{[G]_{\delta_G=0}} = \dot{\psi}_s \cos \kappa_o + \dot{\phi}_s \sin \kappa_o \tag{7}$$

Substituting this expression into equation (6) and making the usual simplifications for small angles gives the equation

$$\dot{\psi}_G = \dot{\psi}_s + \left(\alpha_o - \Phi\right)\dot{\phi}_s + \dot{\theta}\delta_G \tag{8}$$

which is similar to equation (5) except that, for this orientation, the nonlinearity is due to $\dot{\theta}$ rather than $\dot{\phi}_s$. Since, in the derivation of the equations of motion, lateral and longitudinal motions are considered to be independent and $\dot{\theta}$ generally is much less than $\dot{\phi}_s$ in lateral maneuvers, the assumption is made that $\dot{\theta}\delta_G = 0$. Thus, throughout the remainder of this paper the rate-gyro spin axis is considered to be oriented in the direction of the airplane Y-axis. If a future investigation should indicate that the nonlinear term $\delta_G\dot{\phi}_s$ has a negligible effect, the results presented in this paper are applicable to either gyro orientation.

Substitution of equation (8) into equation (3) yields the result (for $\dot{\theta}\delta_G = 0$ and $\ddot{\sigma} = \ddot{\phi}_G$)

$$\left(I_{Y_G} D^2 - M_{\dot{\delta}_G} D - M_{\delta_G}\right)\delta_G = I_{X_G}\omega_{X_G}\left[\dot{\psi}_s + \left(\alpha_o - \Phi\right)\dot{\phi}_s\right] - I_{Y_G}\ddot{\phi}_G \tag{9}$$

where $\ddot{\phi}_G = \ddot{\phi}_s - \left(\alpha_o - \Phi\right)\ddot{\psi}_s$. Since $I_{Y_G} \approx I_{X_G}$, $\omega_{X_G} = 816$ radians per second, and $\left|\ddot{\phi}_G\right| \approx 10\left|\dot{\psi}_G\right|$, the term $I_{Y_G}\ddot{\phi}_G$ should contribute negligibly to the results of this analysis and is omitted.

Relation of gyro-spin-axis deflection to auxiliary-surface deflection.- The deflection of the auxiliary control surface as a function of the gyro-spin-axis deflection δ_G and the hydraulic servo time constant τ is given by

$$(1 + \tau D)\delta_A = K\delta_G \tag{10}$$

The constant K, in terms of the various lengths indicated in figure 1, is

$$K = \frac{ni}{m + n}\frac{z}{wy} \tag{11}$$

The time constant of this servo has been found to have a negligible effect on the results of this analysis and, hence, the assumption is made that $\delta_A = K\delta_G$. For this assumption, equation (9) may be expressed as

$$\left(D^2 + 2\xi\omega_o D + \omega_o^2\right)\delta_A = K_o\omega_o^2\left[\dot{\psi}_s + \left(\alpha_o - \Phi\right)\dot{\phi}_s\right] \tag{12}$$

where $\omega_o^2 = -\frac{M_{\delta_G}}{I_{Y_G}}$ is the damping ratio of the rate gyro $\left(2\xi\omega_o = -\frac{M_{\dot{\delta}_G}}{I_{Y_G}}\right)$, and K_o, which is referred to as the static gearing ratio $\left|\delta_A/\dot{\psi}_G\right|$, is $-\frac{KI_{X_G}\omega_{X_G}}{M_{\delta_G}}$.

For the values of n, i, m, w, y, I_{X_G}, ω_{X_G}, and M_{δ_G} given in table I, the gearing ratio K_o is, as a function of z, $K_o = 2.66\ z$. The range over which z may be varied is from 0 to 3.2 inches; hence, K_o is variable from 0 to approximately 8.5. The maximum deflection of the pump servo arm δ_{ps} (fig. 1) has been measured and found to be $\pm 22.5^\circ$. This deflection is, in terms of the gyro-arm deflection, $\delta_{ps} = \frac{ni}{mh}\delta_G$. For the values of n, i, m, and h given, the pump servo arm is deflected to its maximum value when $\delta_G = \pm 3.24^\circ$. In order to prevent damage to the linkages, stops should be placed on the gyro to limit the gyro deflection to $\pm 3.24^\circ$. From equation (3), it can be seen that δ_G steady state will be equal to 3.24° for $\dot{\psi}_G = 0.125$ radian per second. Therefore, this yaw damper can be expected to operate linearly only if $\dot{\psi}_G$ is less than this value. It should be pointed out, however, that, if the maximum deflection of the control is assumed to be $\pm 20^\circ$, the control would be deflected to its maximum value for $\dot{\psi}_G$ less than 0.125 radian per second if K_o is greater than 2.8. Thus, for higher values of K_o, the maximum value of $\dot{\psi}_G$ for which the yaw damper could be expected to operate linearly would be less than 0.125 radian per second and, hence, for $K_o > 2.8$ the physical limits of the control surface would be more restrictive than the limits on the gyro-spin-axis deflection.

Auxiliary Surface

The auxiliary surface, when deflected, introduces a yawing moment about the airplane Z-axis and a rolling moment about the airplane X-axis; that is,

$$\left(C_n\right)_B = C_{n_{\delta_A}}\delta_A$$

$$\left(C_l\right)_B = C_{l_{\delta_A}}\delta_A$$

The effect of the sideforce introduced by the surface is assumed to be negligible except in the calculation of the yawing and rolling moments produced by the deflection of the surface. The yawing and rolling moments about the stability or flight-path system of axes are related to

the moments about body axes as follows:

$$\left(C_n\right)_S = \left(C_n\right)_B \cos \alpha_o - \left(C_l\right)_B \sin \alpha_o$$

$$\left(C_l\right)_S = \left(C_l\right)_B \cos \alpha_o + \left(C_n\right)_B \sin \alpha_o$$

or, for the assumption of small angles of attack,

$$\left.\begin{aligned} \left(C_{n_{\delta_A}}\right)_S &= \left(C_{n_{\delta_A}}\right)_B - \left(C_{l_{\delta_A}}\right)_B \alpha_o \\ \left(C_{l_{\delta_A}}\right)_S &= \left(C_{l_{\delta_A}}\right)_B + \left(C_{n_{\delta_A}}\right)_B \alpha_o \end{aligned}\right\} \quad (13)$$

The auxiliary surface proposed for use with the yaw damper is shown in figure 3. The surface is to be mounted 13 feet forward of and $2\frac{5}{6}$ feet below the airplane center of gravity on the undersurface of the fuselage, slightly offset to the left of center (looking forward from center of gravity). This offset is necessary in order that the surface not interfere with the lowering and retraction of the nose wheel. The surface is to be hinged at approximately the midpoint of the root chord, and counterclockwise rotation of the surface about its hinge, as seen looking down, is taken as positive rotation; thus, positive deflection of the surface results in a negative sideforce or a negative yawing moment about the airplane Z-axis. This convention is selected in order that K_o be positive for a yaw damper which introduces a yawing moment opposing the airplane yawing velocity. The values of $C_{n_{\delta_A}}$ and $C_{l_{\delta_A}}$ of this surface related to airplane body axes were estimated from the results presented in references 3 and 4 and unpublished data to be -0.01 and 0.0022 per radian, respectively. These values were found to be essentially the same for all flight conditions considered. The values of $C_{n_{\delta_A}}$ and $C_{l_{\delta_A}}$ about stability axes can be determined from equation (13) for each flight condition by substituting the airplane angle of attack and are presented in table II.

EQUATIONS OF MOTION

The equations which describe the lateral motion of the yaw-damper-equipped airplane about stability or flight-path axes are as follows:

Yawing,

$$\left(2\mu_b K_Z^2 \frac{b^2}{V^2} D^2 - \frac{1}{2} C_{n_r} \frac{b}{V} D\right)\psi + \left(2\mu_b K_{XZ} \frac{b^2}{V^2} D^2 - \frac{1}{2} C_{n_p} \frac{b}{V} D\right)\phi -$$

$$C_{n_\beta}\beta = C_{n_{\delta_A}}\delta_A + C_n$$

Rolling,

$$\left(2\mu_b K_{XZ} \frac{b^2}{V^2} D^2 - \frac{1}{2} C_{l_r} \frac{b}{V} D\right)\psi + \left(2\mu_b K_X^2 \frac{b^2}{V^2} D^2 - \frac{1}{2} C_{l_p} \frac{b}{V} D\right)\phi - \qquad (14)$$

$$C_{l_\beta}\beta = C_{l_{\delta_A}}\delta_A + C_l$$

Sideslip,

$$\left(2\mu_b \frac{b}{V} D\right)\psi - C_L\phi + \left(2\mu_b \frac{b}{V} D - C_{Y_\beta}\right)\beta = 0$$

Control,

$$\left(D^2 + 2\xi\omega_o D + \omega_o^2\right)\delta_A - K_o\omega_o^2\left[D\psi + \left(\alpha_o - \Phi\right)D\phi\right] = 0$$

The stability derivatives $C_{Y_{\delta_a}}$, C_{Y_p}, and C_{Y_r} have been neglected in equations (14); also, the equations are for level flight. These equations are assumed to represent the case for which the rate-gyro spin axis is oriented in the direction of the airplane Y-axis, and the gyro Z-axis is at an angle Φ to the airplane Z-axis in the airplane X,Z plane.

The characteristic equation of the airplane yaw-damper system is of the form

$$A\lambda^6 + B\lambda^5 + C\lambda^4 + D\lambda^3 + E\lambda^2 + F\lambda + G = 0 \qquad (15)$$

where the coefficients A, B, C, and so forth for any flight condition of the airplane and given values for the yaw-damper parameters ξ and ω_o can be expressed as functions of the yaw-damper gearing ratio K_o and the gyro Z-axis inclination Φ.

ANALYSIS AND DISCUSSION

Effect of linear yaw damper.- Calculations were made for four cruising conditions at a Mach number equal to 1.6 and two landing conditions of the Douglas D-558-II in an effort to select a yaw-damper gearing ratio K_o and an inclination of the gyro Z-axis to the fuselage Z-axis such that the airplane has satisfactory Dutch roll stability for all the flight conditions considered. The mass and aerodynamic characteristics for each of the investigated flight conditions are presented in table II and were estimated from the results of references 5 and 6 and unpublished wind-tunnel tests at supersonic Mach numbers. For each of flight conditions 1 to 5 (see table II) a boundary was obtained in the K_o, Φ-plane which defined the combinations of K_o and Φ for which the Dutch roll oscillation would damp to one-half amplitude in one period of the oscillation or less, and the results are presented in figure 4. These boundaries were calculated by methods similar to those presented in references 7 and 8. The cross-hatched region shown in the figure defines the combinations of K_o and Φ for which the Dutch roll oscillation of all the flight conditions will damp to one-half amplitude in less than one period, but the values of K_o within this region are so large as to make the region impractical. Satisfactory oscillatory stability can be obtained for flight conditions 1 to 4, however, for much smaller values of K_o. Calculations were made on the Reeves Electronic Analog Computer for cases 1 to 4 in which K_o and Φ were varied systematically and for $K_o = 2.5$ and $\Phi = 2^\circ$ all four cases were very satisfactory. This combination of gearing and inclination was selected on the basis of satisfactory stability and low gearing ratio and because slight variations from these values produce small variation in the system stability. For case 5 and $\Phi = 2^\circ$, a gearing ratio of approximately 6.5 would be necessary for the oscillation to damp to one-half amplitude in one cycle. However, for $K_o = 2.5$ and $\Phi = 2^\circ$, the oscillation of case 5 damps to one-half amplitude in about 1.5 cycles which satisfies the existing Air Force criterion (ref. 2) for period-damping relationship of the lateral oscillation. Thus, if this is considered satisfactory for the landing case, no problem arises. The yaw-damper gearing ratio can be adjusted in the cockpit from 0 to about 8.5; hence, if $C_{1/2} = 1.5$ is not

acceptable for the landing case, the value of K_o can be increased to about 6.5 by the pilot and the stability for this case should then be satisfactory.

The results of the calculations made on the Analog Computer are presented in figure 5 for all six flight conditions for $K_o = 2.5$ and $\Phi = 2^o$. Also, for case 5, motions are shown for $K_o = 6.5$ and $\Phi = 2^o$. For comparison, the motions for the respective flight conditions without yaw damper are also shown, and in every case except case 5 the increase in stability is very apparent. Flight condition 6 is presented, since this condition has been used in flight tests as a means of determining the characteristics of the D-558-II in the landing configuration. The lateral motions for this case without yaw damper are seen to be less stable than those obtained for the true landing case (case 5), but the yaw damper is far more effective in the simulated landing configuration than in the true landing case. The increased effectiveness of the yaw damper for the landing condition at $C_L = 0.36$ (case 6) as compared with that obtained for $C_L = 1.05$ may be attributed, to a large degree, to the higher flight speed for $C_L = 0.36$. This conclusion is based on the fact that this yaw damper essentially increases the damping-in-yaw stability derivative C_{n_r} which generally has a very appreciable stabilizing effect on the stability of the Dutch roll oscillation. The increment to this derivative, if the lags in the yaw damper are negligible, can be shown to be

$$\Delta C_{n_r} = 2K_o C_{n_{\delta_A}} \frac{V}{b}$$

Thus, this increment to C_{n_r} is seen to vary directly with the airspeed V and, for the landing configuration at $C_L = 0.36$ at 12,000 feet, would be approximately twice that obtained for the landing case at $C_L = 1.05$ at sea level or 12,000 feet. It should be pointed out that in these calculations the control deflections were limited to $\pm 20^o$, since this is assumed to be the physical limit on the auxiliary-surface deflection. As was pointed out previously, the gyro-arm deflection is limited to 3.24^o which occurs for $\dot{\psi}_G = \pm 0.125$ radian per second. Hence, the limits on the control deflection for $K_o = 2.5$ should have been approximately $\pm 18^o$, but this slight difference should have a negligible effect on the results presented.

Additional calculations were made to determine the variation of period and damping in the vicinity of $K_o = 2.5$ and $\Phi = 2^o$ for all

six flight conditions and the results are presented in table III. These results are in agreement with those obtained from the previously discussed Analog studies, and for every case except the landing condition at sea level, the Dutch roll oscillation should damp to one-half amplitude in close to, or less than one cycle throughout the range of K_o and Φ considered. The stability characteristics, presented in table III, of the airplane in the landing condition at sea level, although not as desirable as those of the other flight conditions considered, might be considered satisfactory. The primary conclusion which should be reached from the results shown in table III is that values of $K_o = 2.5$ and $\Phi = 2^o$, selected as the optimum combination of control gearing and gyro Z-axis inclination for the investigated flight conditions as a whole, are not critical values since the airplane stability for combinations of K_o and Φ in the vicinity of the chosen values is not appreciably different from that calculated for $K_o = 2.5$ and $\Phi = 2^o$.

Effect of variations in the principal moments of inertia.- The values of $K_{X_o}^2$ and $K_{Z_o}^2$ from which were calculated K_X^2, K_Z^2, and K_{XZ} for the various flight conditions were obtained from data presented in reference 5. More recent data on the airplane principal moments of inertia which were provided by the NACA High-Speed Flight Research Station at Edwards Air Force Base, Calif. (referred to herein as HSFRS), differed considerably from those of reference 5 and for purposes of comparison both sets of values are presented in figure 6 plotted against wing loading W/S. Throughout the calculations, the assumption is made that the principal longitudinal axis is located 3.7^o below the fuselage axis and is invariant with wing loading. Calculations were made for each of flight conditions 1 to 6 in which the moments of inertia afforded by HSFRS were utilized. The results of these calculations indicated no appreciable effect of the assumed variations in the inertial moments and are not presented, but it may be of interest to note that the largest effects were obtained for the landing configurations.

SUGGESTIONS FOR FUTURE RESEARCH

A more detailed analysis of the effects of the various nonlinearities in the yaw-damper system, such as Coulomb friction, operation of the control surface at full deflection, and pitching of the gyro spin axis following airplane rotational velocities, should be made. Also, the effect of these nonlinearities on the airplane response characteristics following various inputs should be investigated.

CONCLUDING REMARKS

An analysis made to determine the effect of a yaw damper, designed and constructed by the Flight Research Division, on the Dutch roll stability of the Douglas D-558-II research airplane indicates that this yaw damper, when used in conjunction with the auxiliary control surface described in this paper, should be capable of improving markedly the inherently poor stability of the airplane. Calculations made for several representative flight conditions indicate that satisfactory stability should be obtained for the high-speed flight conditions for a control gearing of 2.5 when the gyro gimbal axis is inclined 2° nose down relative to the airplane X-axis, but the stability is marginal for the landing configuration at sea level. If better stability is desired for the landing case a gearing ratio of 6.5 should be used for this gyro-axis inclination.

A preliminary phase of the analysis showed that the rate-gyro spin-axis deflection varied nonlinearly with airplane rate of roll about the stability X-axis if the gyro spin axis was oriented along the direction of the airplane X-axis but varied linearly with rate of roll if the spin axis was oriented along the airplane Y-axis. For this reason, the gyro spin axis was assumed to be oriented along the airplane Y-axis for all the calculations presented in this paper.

If the control gearing is to be variable in the cockpit from 0 to 8.5, stops should be placed on the gyro to limit its deflection to approximately $\pm 3\frac{1}{4}^{\circ}$ so as to prevent damage to the linkages.

Langley Aeronautical Laboratory,
National Advisory Committee for Aeronautics,
Langley Field, Va.

REFERENCES

1. Gates, Ordway B., Jr., and Sternfield, Leonard: Effect of an Autopilot Sensitive to Yawing Velocity on the Lateral Stability of a Typical High-Speed Airplane. NACA TN 2470, 1951.

2. Anon.: Flying Qualities of Piloted Airplanes. U.S. Air Force Specification No. 1815-B, June 1, 1948.

3. Martin, John C., and Malvestuto, Frank S., Jr.: Theoretical Force and Moments Due to Sideslip of a Number of Vertical Tail Configurations at Supersonic Speeds. NACA TN 2412, 1951.

4. DeYoung, John, and Harper, Charles W.: Theoretical Symmetric Span Loading at Subsonic Speeds for Wings Having Arbitrary Plan Form. NACA Rep. 921, 1948.

5. Queijo, M. J., and Goodman, Alex: Calculations of the Dynamic Lateral Stability Characteristics of the Douglas D-558-II Airplane in High-Speed Flight for Various Wing Loadings and Altitudes. NACA RM L50H16a, 1950.

6. Queijo, M. J., and Wells, Evalyn G.: Wind-Tunnel Investigation of the Low-Speed Static and Rotary Stability Derivatives of a 0.13-Scale Model of the Douglas D-558-II Airplane in the Landing Configuration. NACA RM L52G07, 1952.

7. Sternfield, Leonard, and Gates, Ordway B., Jr.: A Method of Calculating a Stability Boundary That Defines a Region of Satisfactory Period-Damping Relationship of the Oscillatory Mode of Motion. NACA TN 1859, 1949.

8. Brown, W. S.: A Simple Method of Constructing Stability Diagrams. R. & M. No. 1905, British A.R.C., 1942.

TABLE I

YAW-DAMPER PARAMETERS

I_{X_G}, slug-ft^2	0.00765
I_{Y_G}, slug-ft^2	0.0090
M_{δ_G}, ft-lbs/radian	-13.8
$M_{\dot{\delta}_G}$, ft-lbs/radian/sec	-0.386
Yaw-damper lever-arm lengths, in.:	
z	variable
n	5.0
i	5.0
m	1.8
w	0.625
x	3.0
y	1
h	2
ω_{X_G}, radians/sec	816
ξ	0.55
ω_o, radians/sec	39

TABLE II

STABILITY DERIVATIVES AND MASS CHARACTERISTICS USED IN CALCULATIONS OF LATERAL STABILITY OF D-558-II

	Flight condition and configuration					
	I Clean	II Clean	III Clean	IV Clean	V Landing	VI Landing
L/W	1	0.2	1	0.2	1	1
C_L	0.473	0.095	0.184	0.037	1.05	0.36
μ_b	707	707	275	275	33	47.5
ϵ, deg	3.7	3.7	3.7	3.7	3.7	3.7
α_o, deg	6.6	0.28	1.8	-0.7	-9.7	-1.7
η, deg	2.9	-3.42	-1.9	-4.4	6	-5.4
K_X^2	0.015711	0.015833	0.015534	0.016116	0.016729	0.016772
K_Z^2	0.13669	0.13657	0.13687	0.13628	0.13567	0.13563
K_{XZ}	0.0061141	-0.0072056	-0.0040093	-0.0092559	0.012579	-0.011336
C_{n_β}	0.087	0.087	0.087	0.087	0.23	0.29
C_{l_β}	-0.035	-0.067	-0.057	-0.074	-0.20	-0.15
C_{Y_β}	-0.726	-0.726	-0.726	-0.726	-1.15	-1.43
C_{n_r}	-0.50	-0.54	-0.51	-0.56	-0.63	-0.56
C_{l_r}	0.076	0.143	0.122	0.159	0.13	0.17
C_{Y_r}	0	0	0	0	0	0
C_{n_p}	-0.045	-0.0084	-0.017	-0.004	-0.17	-0.06
C_{l_p}	-0.25	-0.25	-0.25	-0.25	-0.33	-0.31
C_{Y_p}	0	0	0	0	0	0
tan γ	0	0	0	0	0	0
V, ft/sec	1553	1553	1553	1553	225	460
S, ft^2	175	175	175	175	175	175
b, ft	25	25	25	25	25	25
W, lbs	14,000	14,000	14,000	14,000	11,000	11,000
Alt., ft	70,000	70,000	50,000	50,000	0	12,000
Mach number	1.6	1.6	1.6	1.6	0.20	0.43
W/S	80	80	80	80	63	63
$\left(C_{n_{\delta_A}}\right)_S$	-0.01	-0.01	-0.01	-0.01	-0.01	-0.01
$\left(C_{l_{\delta_A}}\right)_S$	0.001	0.0022	0.0019	0.0023	0.0005	0.0025

NACA

TABLE III

VARIATION OF PERIOD AND DAMPING WITH Φ AND K_o FOR THE VARIOUS FLIGHT CONDITIONS CONSIDERED

Φ, deg	K_o	Aperiodic Modes		Oscillatory Modes		$C_{1/2}$
		$T_{1/2}$	$T_{1/2}$	$T_{1/2}$	P	
(a) Case 1						
-	0	89.4	1.80	13.5	4.30	3.14
0	2.5	12.1	1.49	3.40	4.43	.77
				.033	.197	.17
1	2.5	11.5	1.56	3.16	4.44	.71
				.033	.197	.17
2	2.5	10.9	1.65	2.95	4.45	.66
				.033	.197	.17
3	2.5	10.3	1.74	2.77	4.46	.62
				.033	.197	.17
2	2.0	13.0	1.68	3.54	4.43	.80
				.033	.197	.17
2	2.5	10.9	1.65	2.95	4.45	.66
				.033	.197	.17
2	3.0	9.4	1.61	2.53	4.48	.57
				.033	.197	.17
(b) Case 2						
-	0	41.90	1.08	-7.30	5.51	-1.30
0	2.5	4.74	1.16	7.39	5.80	1.27
				.033	.197	.17
1	2.5	4.04	1.33	5.56	5.91	.94
				.033	.197	.17
2	2.5	3.17	1.64	4.38	6.01	.73
				.033	.197	.17
3	2.5	-----	----	3.54	6.11	.58
				2.40	61.42	.04
				.033	.197	.17
2	2.0	4.76	1.38	6.63	5.86	1.13
				.033	.197	.17
2	2.5	3.17	1.64	4.38	6.01	.73
				.033	.197	.17
2	3.0	-----	----	3.22	6.20	.52
				2.21	51.96	.043
				.033	.197	.17

TABLE III

VARIATION OF PERIOD AND DAMPING WITH Φ AND K_o FOR THE VARIOUS FLIGHT CONDITIONS CONSIDERED

Φ, deg	K_o	Aperiodic Modes		Oscillatory Modes		$C_{1/2}$
		$T_{1/2}$	$T_{1/2}$	$T_{1/2}$	P	
(c) Case 3						
-	0	45.50	0.59	629	3.15	200
0	2.5	6.24	.52	1.43	3.28	0.44
				.034	.198	.17
1	2.5	5.66	.56	1.27	3.34	.38
				.034	.198	.17
2	2.5	5.07	.62	1.13	3.40	.33
				.034	.198	.17
3	2.5	4.45	.70	1.01	3.46	.29
				.034	.198	.17
2	2.0	6.38	.61	1.42	3.31	.43
				.034	.198	.17
2	2.5	5.07	.62	1.13	3.40	.33
				.034	.198	.17
2	3.0	4.13	.63	.93	3.53	.26
				.034	.199	.17
(d) Case 4						
-	0	30.2	0.46	-4.20	3.57	-1.18
0	2.5	3.404	.46	1.96	4.03	.49
				.034	.198	.17
1	2.5	2.78	.52	1.57	4.25	.37
				.034	.198	.17
2	2.5	2.05	.66	1.25	4.53	.28
				.034	.199	.17
3	2.5	------	----	.957	4.84	.198
				1.27	35.26	.036
				.034	.199	.17
2	2.0	3.22	.56	.18	4.16	.43
				.034	.198	.17
2	2.5	2.05	.66	1.25	4.53	.28
				.034	.199	.17
2	3.0	------	----	.885	5.16	.17
				1.15	21.94	.052
				.034	.199	.17

TABLE III

VARIATION OF PERIOD AND DAMPING WITH Φ AND K_o FOR THE VARIOUS FLIGHT CONDITIONS CONSIDERED

Φ, deg	K_o	Aperiodic Modes		Oscillatory Modes		$C_{1/2}$
		$T_{1/2}$	$T_{1/2}$	$T_{1/2}$	P	
(e) Case 5						
-	0	8.45	0.42	6.87	3.13	2.2
0	2.5	4.68	.41	4.69	3.11	1.51
				.033	.196	.17
1	2.5	4.63	.41	4.51	3.11	1.45
				.033	.196	.17
2	2.5	4.59	.41	4.35	3.12	1.39
				.033	.196	.17
3	2.5	4.54	.42	4.19	3.13	1.34
				.033	.196	.17
2	2.0	5.04	.42	4.69	3.12	1.50
				.033	.196	.17
2	2.5	4.59	.41	4.35	3.12	1.39
				.033	.196	.17
2	3.0	4.21	.41	4.05	3.12	1.30
				.033	.196	.17
(f) Case 6						
-	0	31.9	0.26	-15.3	2.4	-6.4
0	2.5	10.2	.27	2.90	2.4	1.2
				.033	.197	.17
1	2.5	10.1	.27	2.75	2.4	1.13
				.033	.197	.17
2	2.5	9.99	.27	2.61	2.44	1.07
				.033	.197	.17
3	2.5	9.87	.27	2.49	2.45	1.02
				.033	.197	.17
2	2.0	11.66	.27	3.43	2.42	1.42
				.033	.197	.17
2	2.5	9.99	.27	2.61	2.44	1.07
				.033	.197	.17
2	3.0	8.71	.27	2.11	2.45	.86
				.033	.197	.17

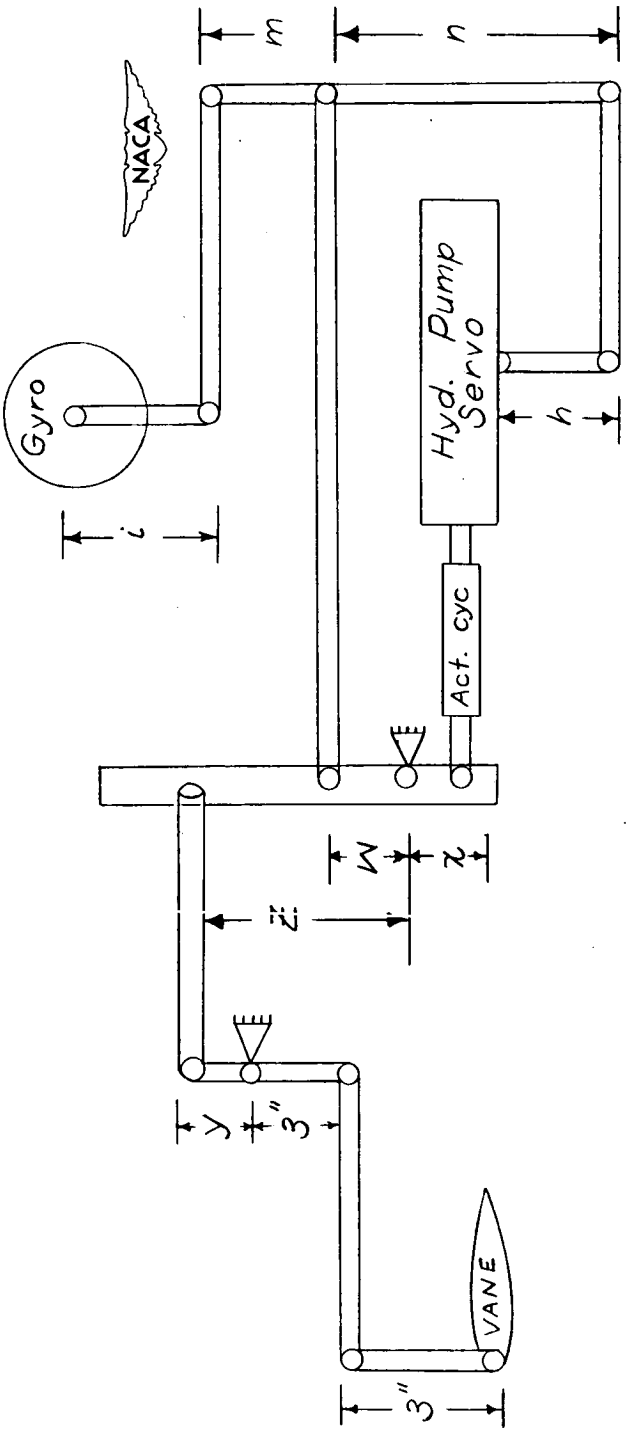

Figure 1.- Sketch of yaw-damper system.

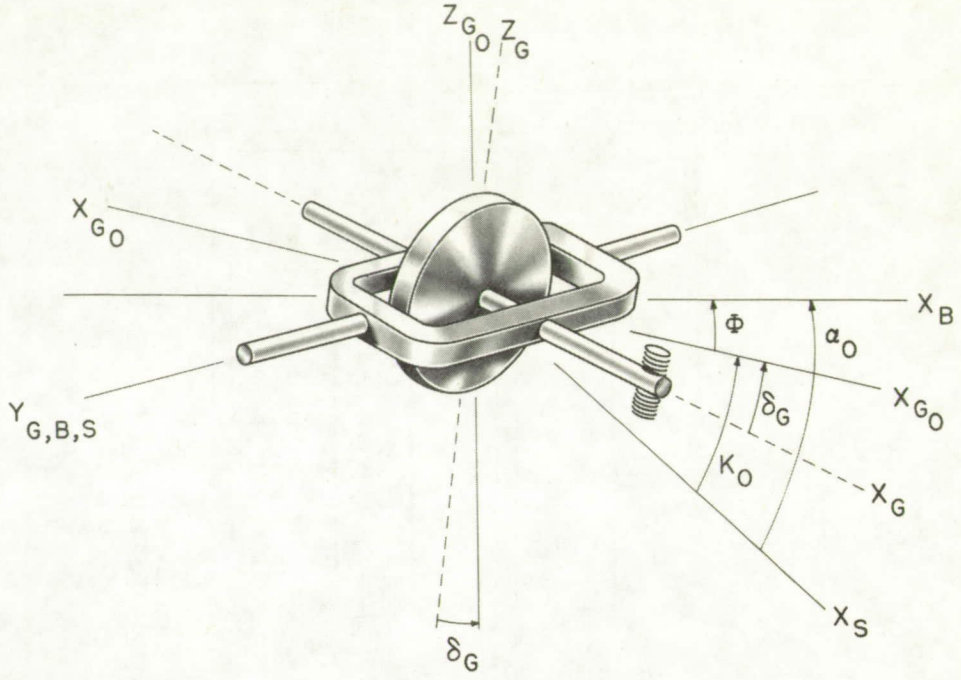

(a) Gyro spin axis oriented in direction of airplane X-axis.

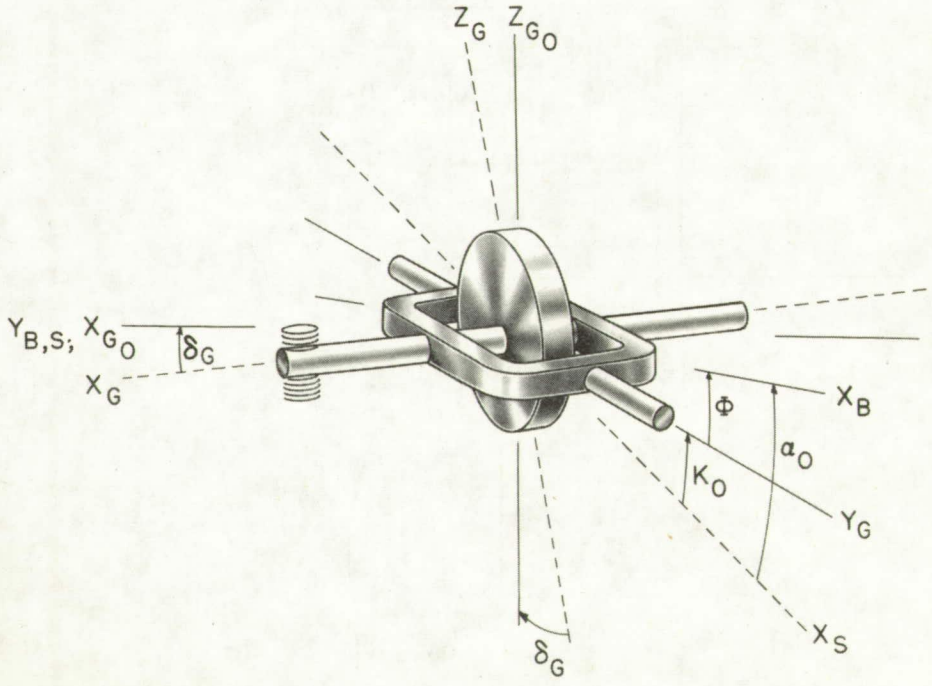

(b) Gyro spin axis oriented in direction of airplane Y-axis.

Figure 2.- System of axes used in analysis.

NACA L-77031

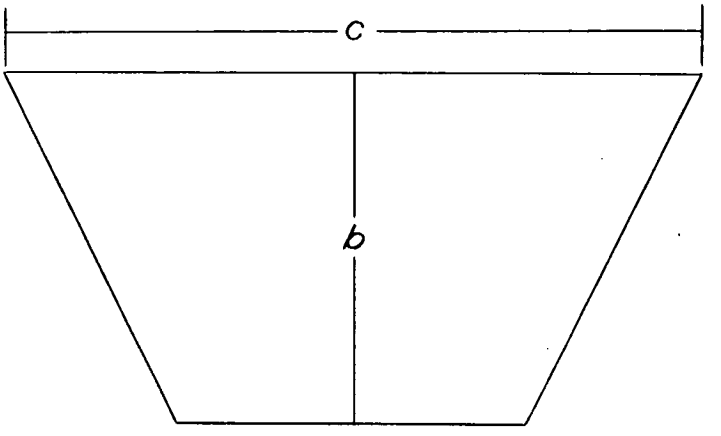

Taper ratio	0.50
Aspect ratio	0.67
Span, b, ft	1.33
Chord, c, ft	2.67
Area, ft^2	2.67
ℓ, ft	13.00
h, ft	2.83

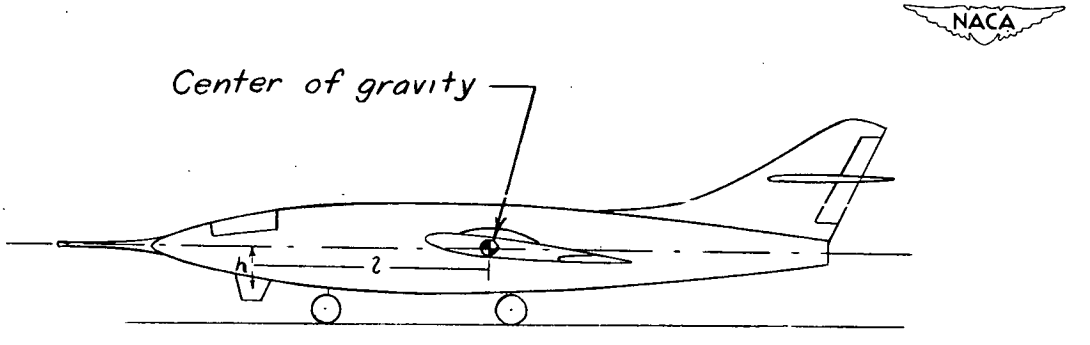

Figure 3.- Sketch of vane proposed for use with yaw damper.

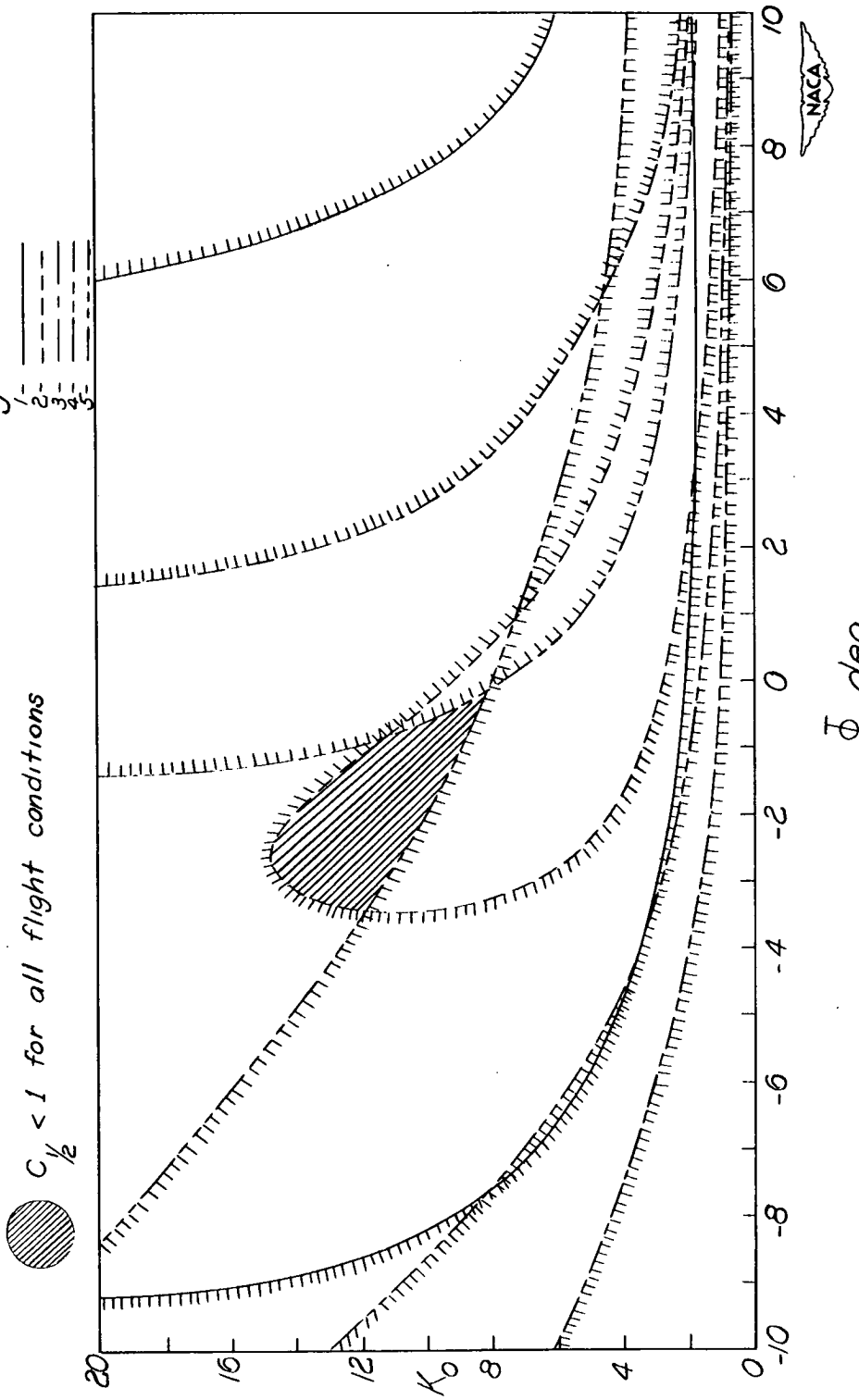

Figure 4.- Boundary which defines the combinations of K_o and Φ necessary for $C_{l/2} \leq 1$ for flight conditions 1 to 5.

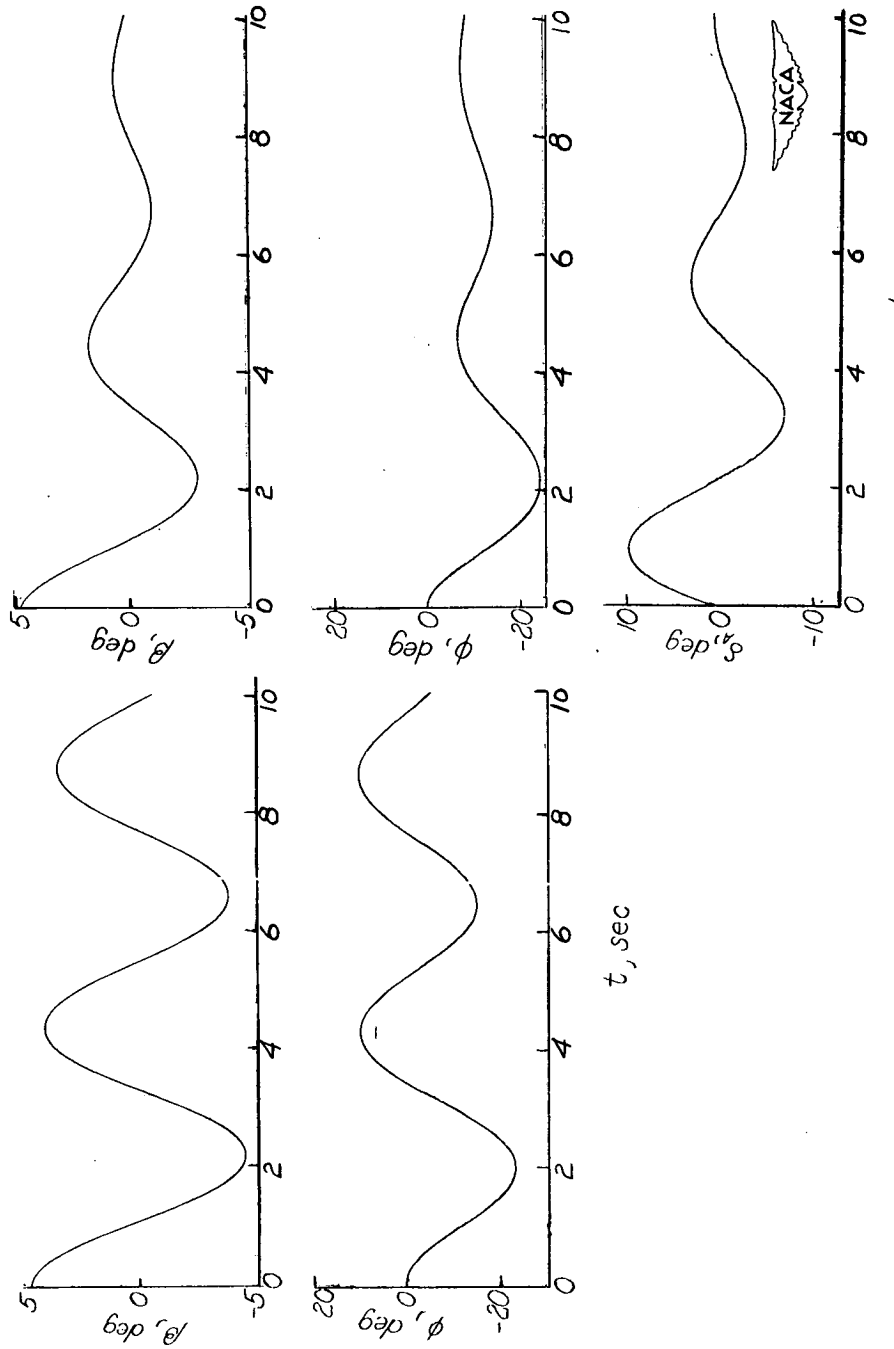

(a) Case 1. Time histories with yaw damper on right; $K_o = 2.5$.

Figure 5.- Lateral motions of the Douglas D-558-II subsequent to a 5° disturbance in sideslip, with and without yaw damper, for the various flight conditions considered. $\Phi = 2°$.

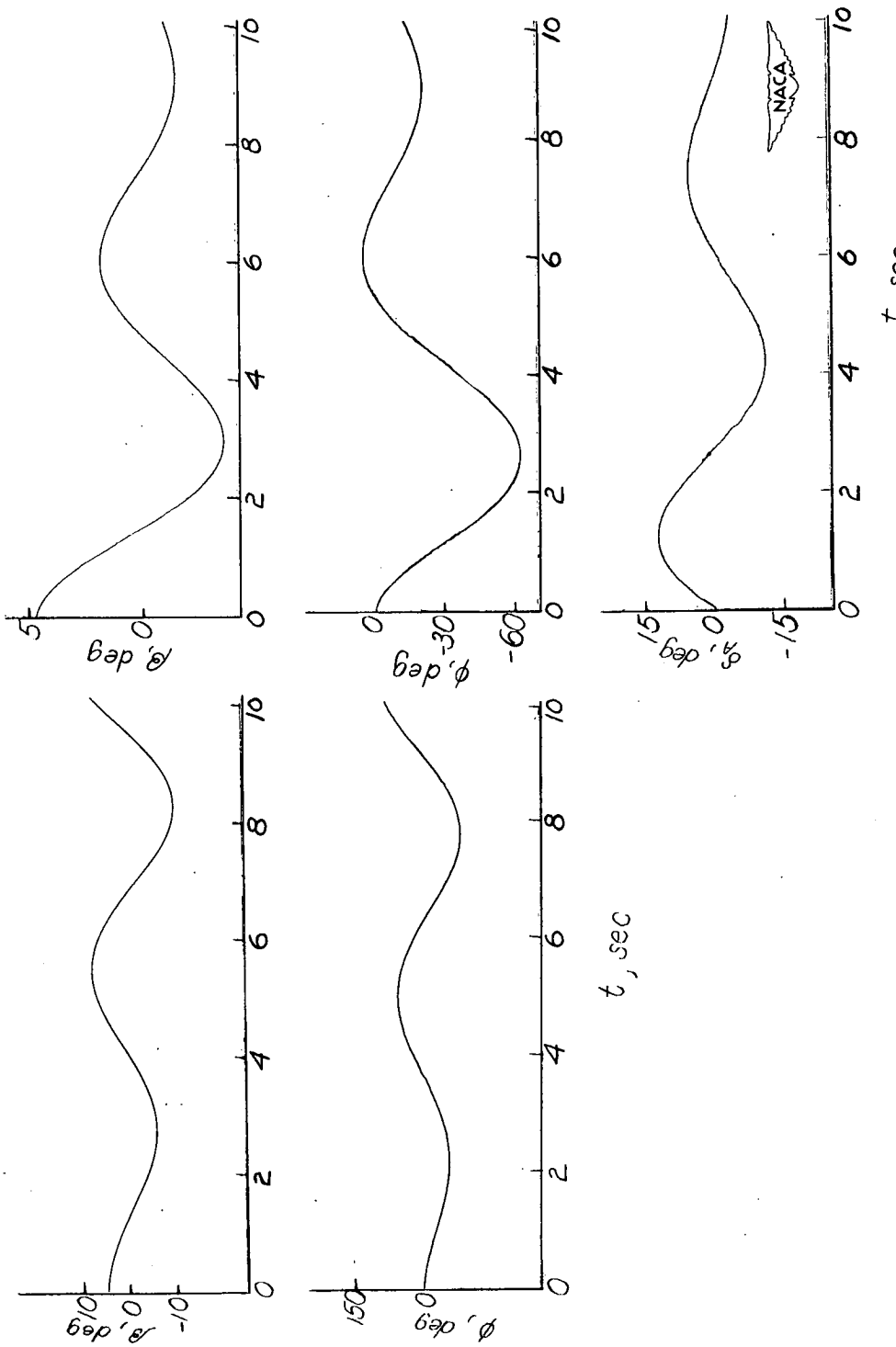

(b) Case 2. Time histories with yaw damper on right; $K_o = 2.5$.

Figure 5.- Continued.

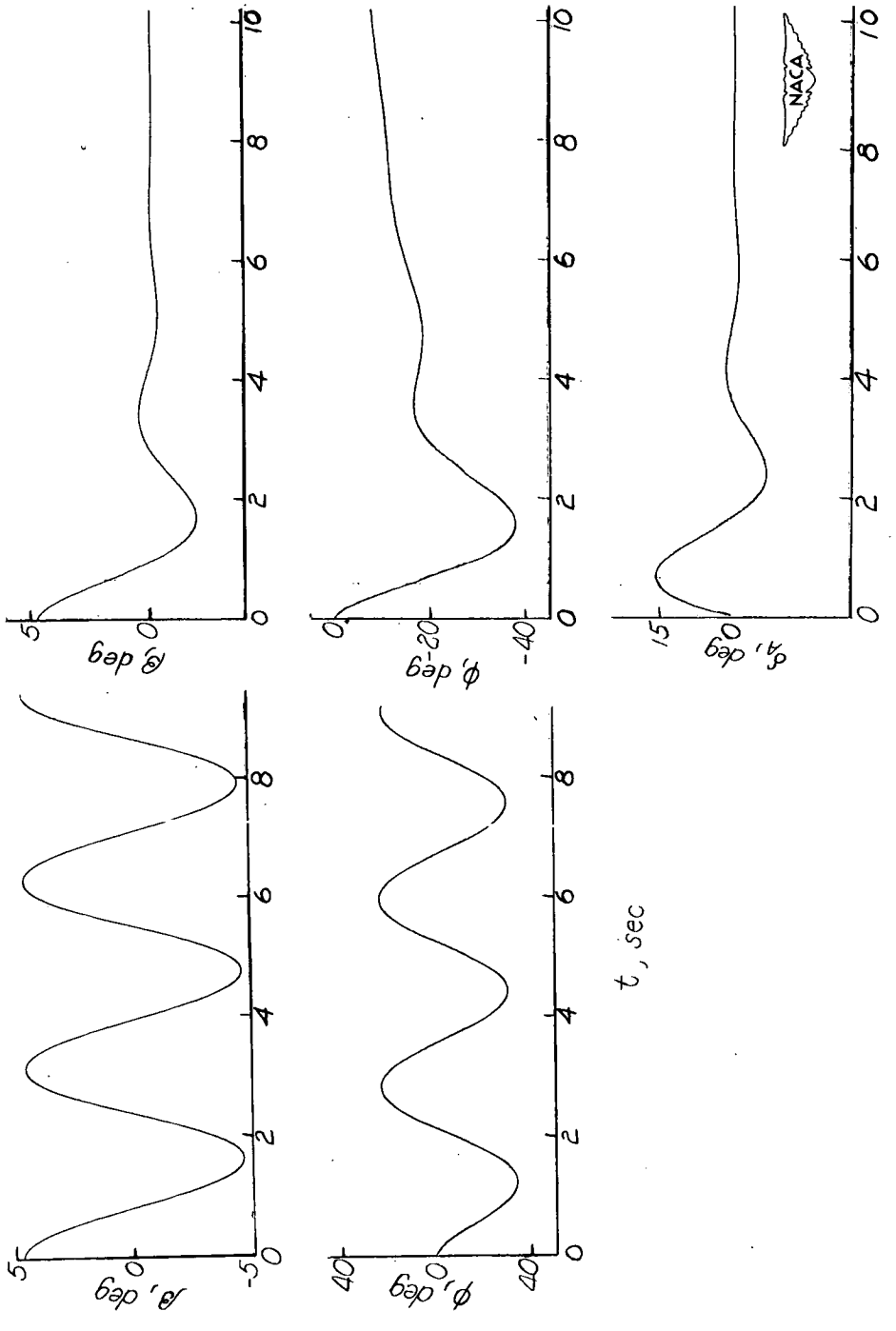

(c) Case 3. Time histories with yaw damper on right; $K_O = 2.5$.

Figure 5.- Continued.

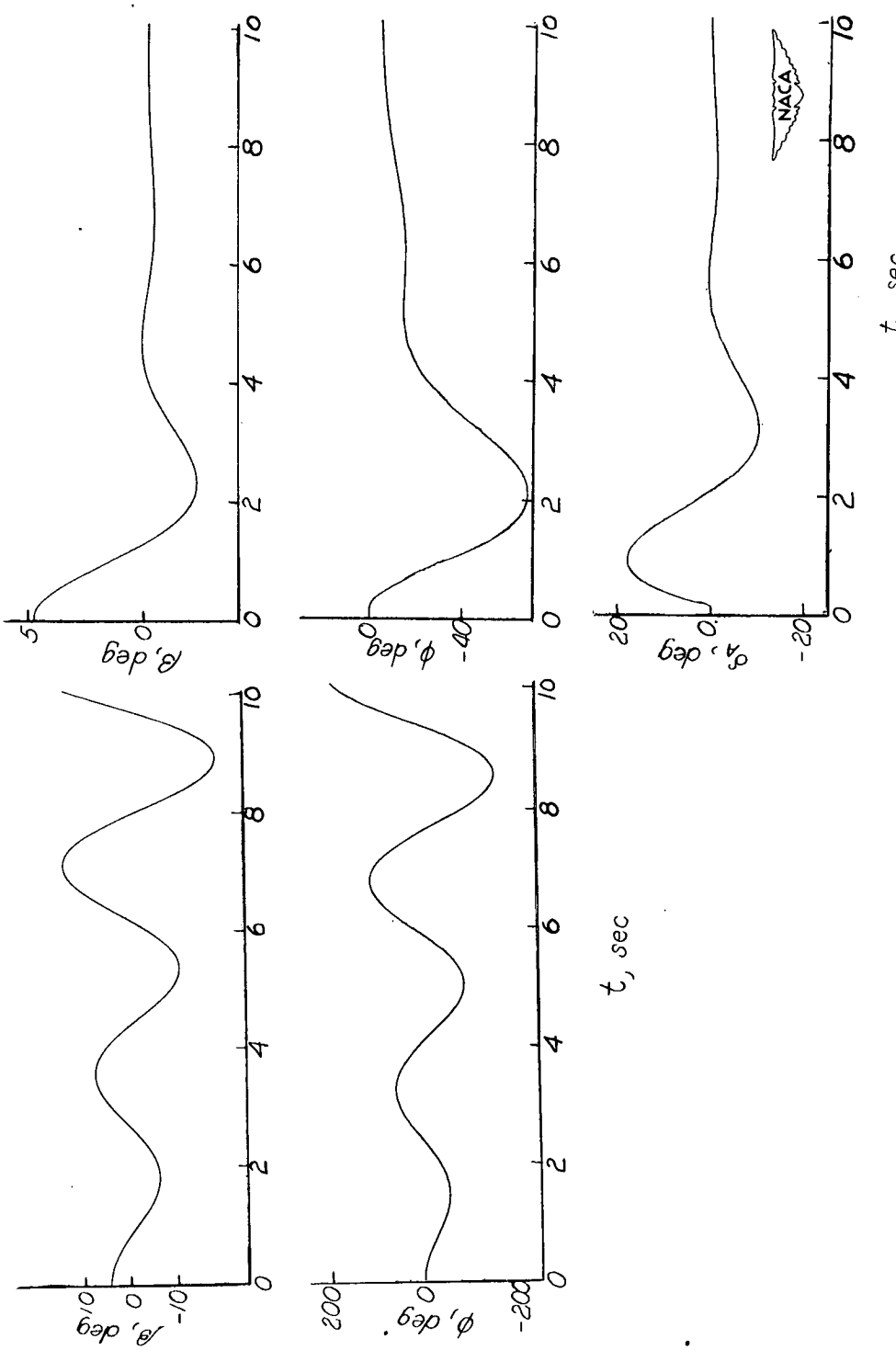

(d) Case 4. Time histories with yaw damper on right; K_O = 2.5.

Figure 5.- Continued.

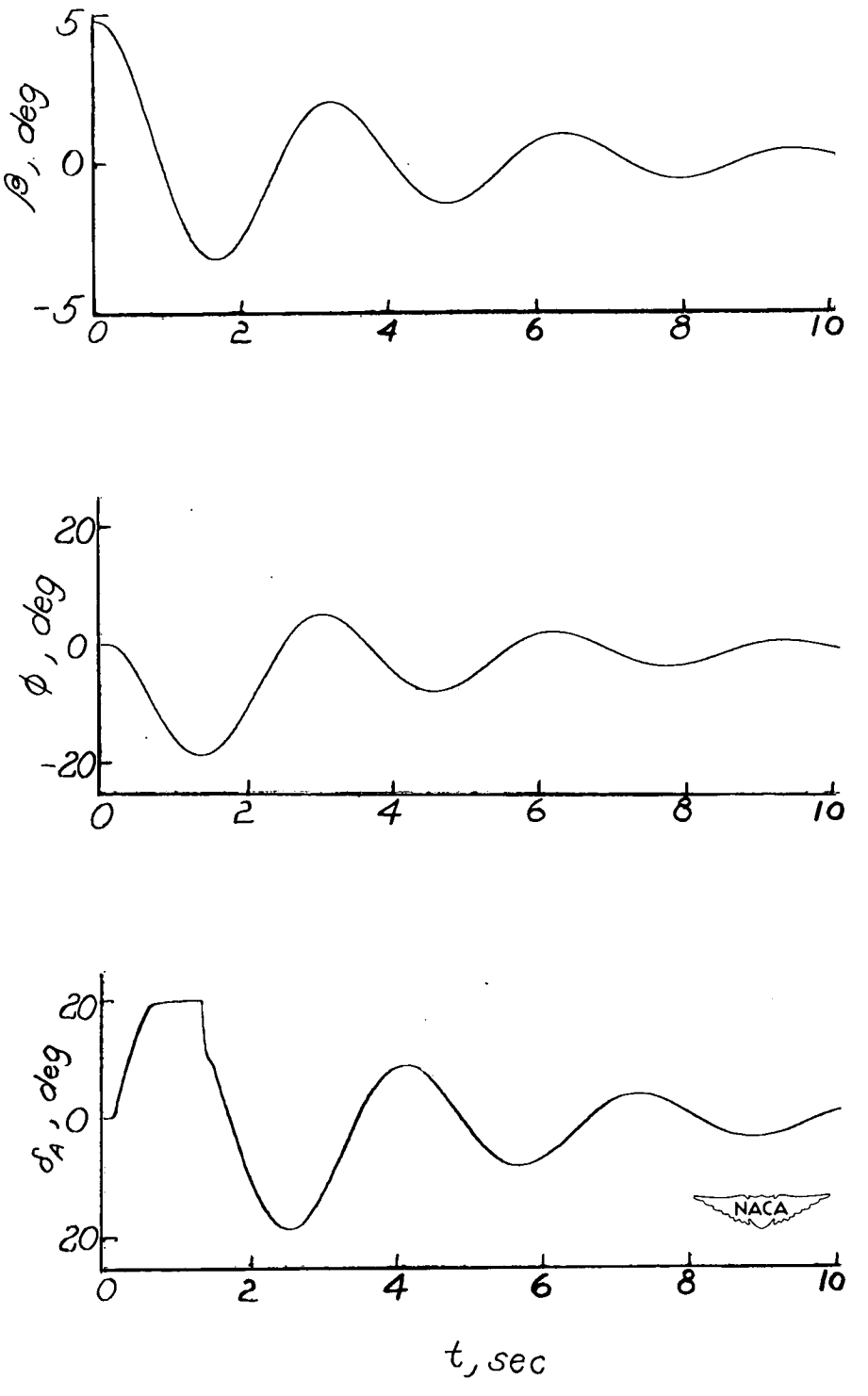

(f) Case 5. With yaw damper; K_O = 6.5.

Figure 5.- Continued.

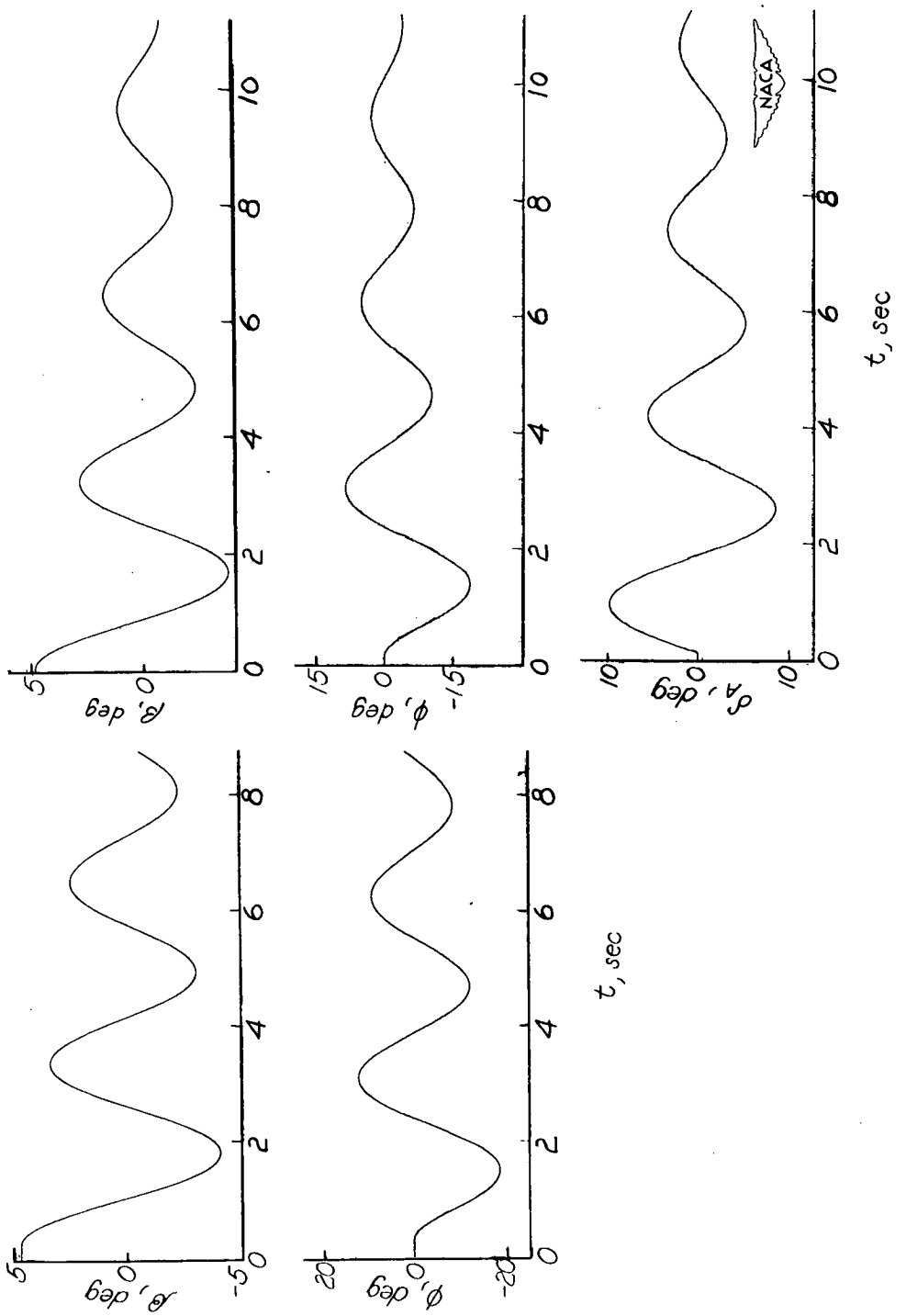

(e) Case 5. Time histories with yaw damper on right; $K_O = 2.5$.

Figure 5.- Continued.

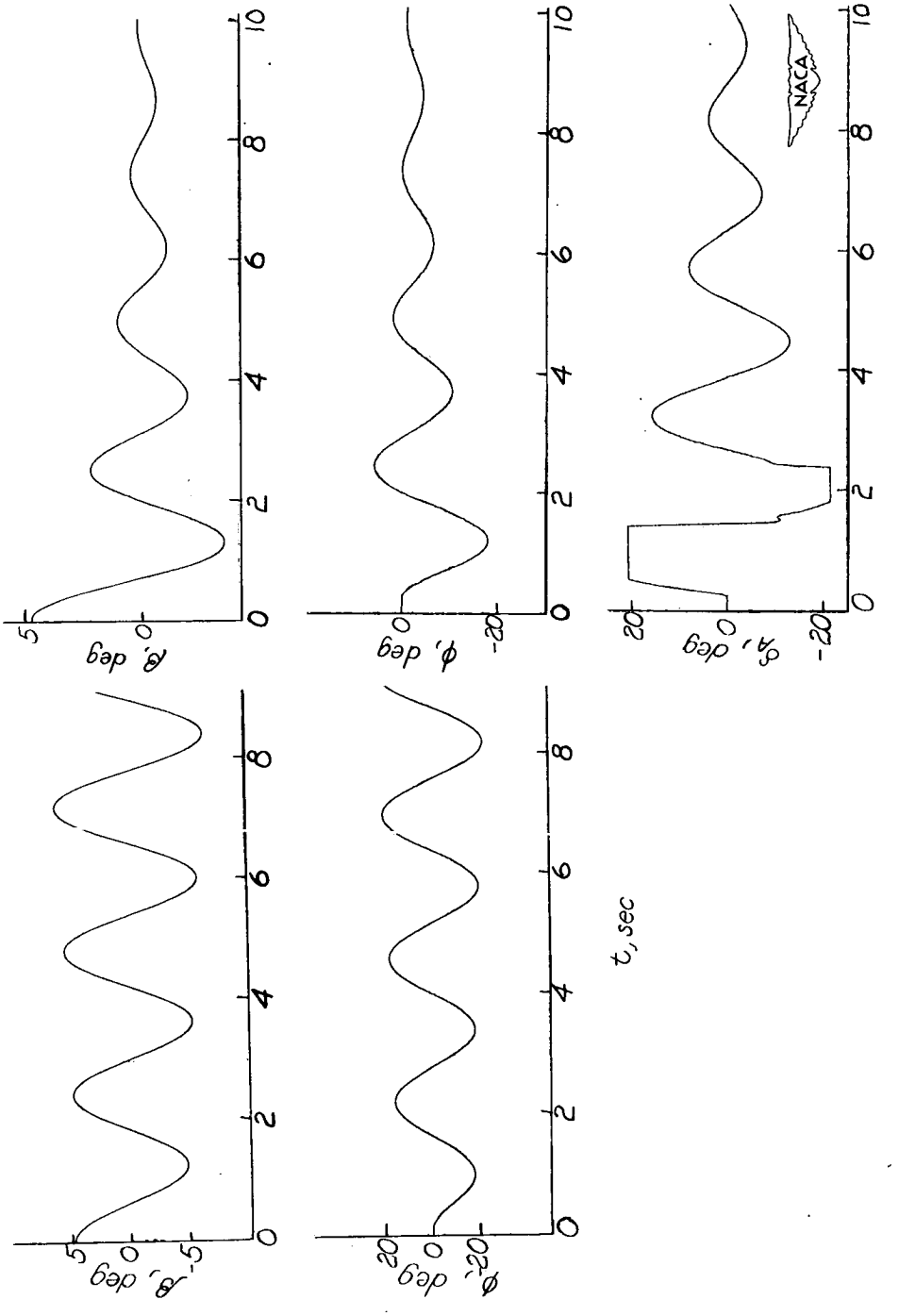

(g) Case 6. Time histories with yaw damper on right; K_D = 2.5.

Figure 5.- Concluded.

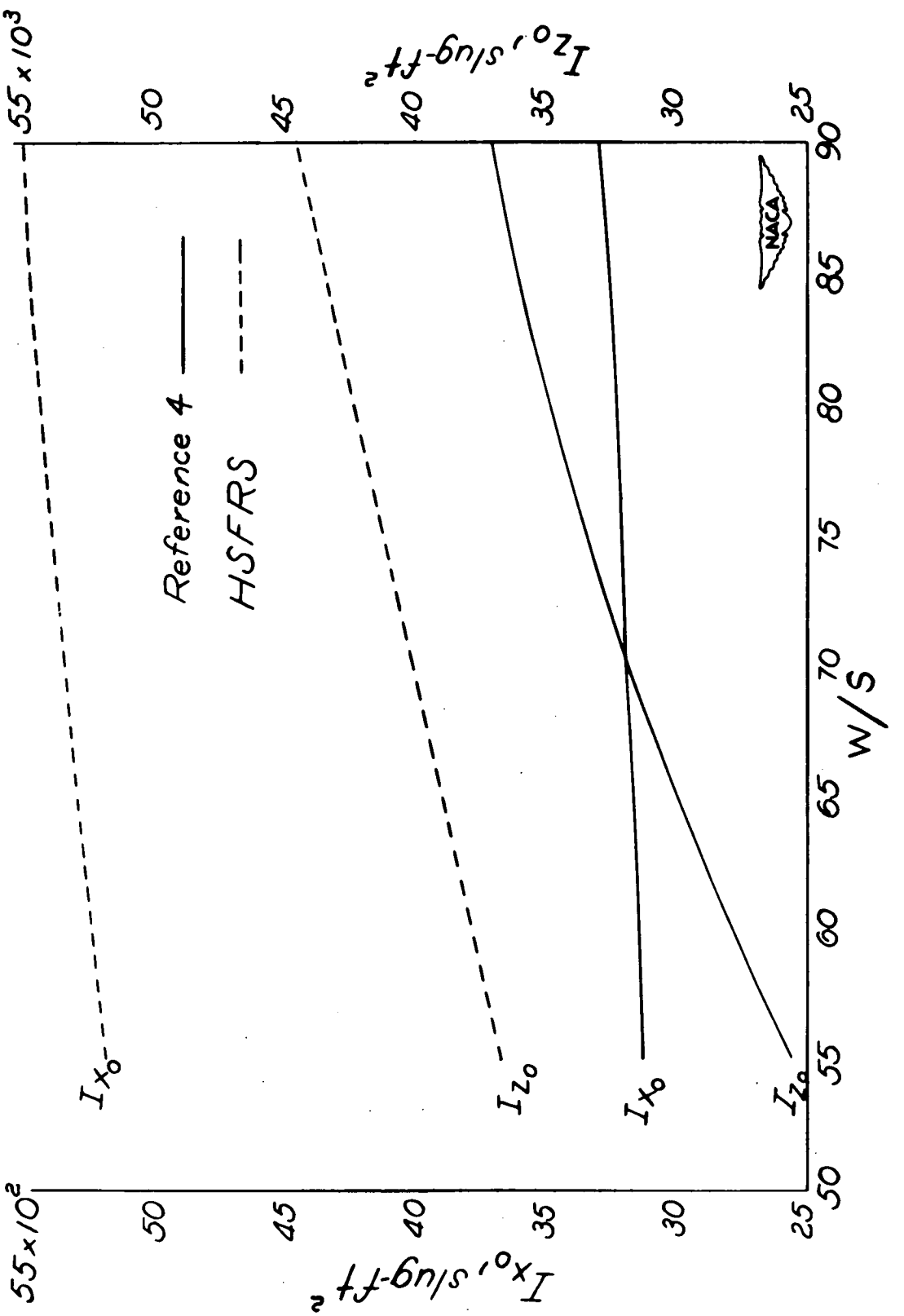

Figure 6.- Variation of moments of inertia of the Douglas D-558-II with wing loading.